МОДЕЛЮВАННЯ ТА ОПТИМІЗАЦІЯ В ТЕХНОЛОГІЇ КОНСТРУКЦІЙНИХ МАТЕРІАЛІВ

SIMULATION AND OPTIMIZATION IN TECHNOLOGY OF CONSTRUCTION MATERIALS

DOI: 10.31319/2519-8106.1(50)2024.305037
UDC 622.673.1

Kovyriev Maksym, postgraduate student, Department of engineering and design in machinery industry
Ковирєв М.В., здобувач третього (доктора філософії) рівня вищої освіти, кафедра інжинірингу та дизайну в машинобудуванні,
ORCID: 0000-0002-3250-9499
e-mail: Kovyriev.M.V@nmu.one

Zabolotnyi Kostiantyn, Doctor of Technical Sciences, Professor, Head of the Engineering and Design in Machinery Industry Department
Заболотний К.С., доктор технічних наук, професор, завідувач кафедри інжинірингу та дизайну в машинобудуванні,
ORCID: 0000-0001-8431-0169
e-mail: zabolotnyi.k.s@nmu.one

Panchenko Olena, Candidate of Technical Sciences, Associate Professor, Department of engineering and design in machinery industry
Панченко О.В., кандидат технічних наук, доцент, кафедра інжинірингу та дизайну в машинобудуванні
ORCID: 0000-0002-1664-2871
e-mail: panchenko.o.v@nmu.one

Kukhar Viktor, Candidate of Technical Sciences, Associate Professor, Department of engineering and design in machinery industry
Кухар В.Ю., кандидат технічних наук, доцент, кафедра інжинірингу та дизайну в машинобудуванні
ORCID: 0000-0002-1849-4489
e-mail: kukhar.v.yu@nmu.one

National Technical University "Dnipro Polytechnic", Dnipro
Національний технічний університет «Дніпровська політехніка», м. Дніпро

DEVELOPMENT OF A MODEL OF RUBBER ROPE IN MULTILAYER WINDING AS A COMPOSITE MATERIAL

РОЗРОБКА МОДЕЛІ БАГАТОШАРОВОЇ НАМОТКИ КАНАТА ІЗ КОМПОЗИТНОГО МАТЕРІАЛУ

The proposed article is devoted to an important scientific task — clarifying the force loads in the coils of the multilayer winding of rubber-tether ropes of spool hoists. The aim of the study is to develop a mathematical model of the stress-strain state of the winding body of a spool hoist with a

rubber-tether rope. The methods of mathematical and computational experiment based on finite element analysis were used in the study. When solving the problem of determining the stiffness of the body of a rubber-tether rope (RTR) winding, the physical model of its spool body was represented as a composite, where the rope reinforcement is considered to be an infinitely thin spiral with the stiffness characteristics of a metal cable, and the matrix is a rubber sheath. After processing the results of a computational experiment to determine the parameters of the RTW winding body, carried out by computer finite element modeling, an analytical expression was obtained to calculate its stiffness coefficient, which suggests a quadratic relationship between the stiffness of the winding body and its outer diameter, with the local stiffness of the structure depending insignificantly on the diameter value. The danger of dynamic effects in hoist spools can occur when the winding has many turns. The regularities of the influence of the parameters of a rubber rope on the torsional stiffness of its winding body have been established. The nonlinear nature of the change in the considered stiffness characteristics of each winding layer in the RTW package is caused by the peculiarity of the interaction of the first layer with the surface of the spool. This interaction can be traced by applying the torsional stiffness gain factor calculated using the analytical expression obtained by processing the results of the computational experiment. The developed mathematical model for determining the torsional stiffness of a rubber rope winding makes it possible to find such values of the parameters of a spool hoist that will avoid the danger of dynamic effects during emergency and operational braking of the device caused by the torsional stiffness of the winding body.

***Keywords**: methods of rating of forcing factors, rubberrope cable, multilayer winding, the body of the winding, longitudinal and diametrical cable hardness, bobbin hoisting machine.*

Запропонована стаття присвячена важливому науковому завданню — уточнення силових навантажень у витках багатошарової намотки гумотросових канатів бобінних підйомників. Мета дослідження — розробка математичної моделі напружено-деформованого стану тіла намотки бобінних підіймальних машин з гумотросовим канатом. У роботі використано методи математичного та обчислювального експерименту на основі скінченно-елементного аналізу. Розв'язуючи задачі на визначення жорсткості тіла намотки гумотросового каната (ГТК), фізичну модель її бобінного органа уявили у вигляді композиту, де армування каната вважається нескінченно тонкою спіраллю з жорсткісними характеристиками металевого троса, а матриця — гумовою оболонкою. Після обробки результатів обчислювального експерименту з визначення параметрів тіла намотки ГТК, здійсненого методом комп'ютерного скінченно-елементного моделювання, отримали аналітичний вираз для розрахунку її коефіцієнта жорсткості, із якого випливає висновок про квадратичну залежність між жорсткістю тіла намотки та її зовнішнім діаметром, причому локальна жорсткість конструкції від значення діаметра залежить несуттєво. Небезпека виникнення в бобінах підйомника динамічних ефектів, може мати місце, коли намотка має багато витків. Встановлено закономірності впливу параметрів гумотросового каната на крутильну жорсткість тіла його намотки. Нелінійний характер зміни розглянутих характеристик жорсткості кожного шару намотки в пакеті ГТК викликаний особливістю взаємодії першого шару з поверхнею бобіни. Цю взаємодію можна простежити, застосовуючи коефіцієнт посилення жорсткості на кручення, обчислюваний за допомогою отриманого шляхом обробки результатів обчислювального експерименту аналітичного виразу. Розроблена математична модель визначення жорсткості намотки гумотросового каната дозволяє знаходити такі значення параметрів бобінного підйомника, що дозволять уникнути небезпеки появи динамічних ефектів під час аварійного та робочого гальмування пристрою, викликаних крутильною жорсткістю тіла намотки.

***Ключові слова**: метод розрахунку силових факторів, гумотросовий канат, багатошарова намотка, тіло намотки, поздовжня та поперечна жорсткість каната, бобінна піднімальна машина.*

Analysis of recent research and publications

Currently, there is a need to create powerful lifts to depths of over 1500 meters. Specialists of NTU "SE", "Kryvbasproekt", NKMZ, Polyakov Research Institute of Mechanical Engineering proposed to use rubber-tether tapes and ropes (RTT, RTR) with dense packing as a traction body, which

with an end load of up to 160 tons allow for vertical lifting of cargo up to 1700 m with a belt width of 1.65 m. prof. Kolosov and his followers theoretically and practically substantiated the creation of reel hoisting systems with RTRs and the same systems with friction pulleys [1, 2] for vertical mines, quarries and offshore mining [3, 4].

In a spool hoist, there is a multilayer rubber-tether rope winding, a new, unexplored element of the hoisting system with great pliability [5, 6]. This pliability is due to the rubber of the tape and consists of shear, torsional, and compression deformations of the RTT turns. The occurrence of such pliability can lead to unpleasant phenomena in the operating and emergency modes of operation of the reel hoist, namely: destruction of the rope, reel, and flange from the load caused by the multilayer winding under the operating tension of the rope in the reel, as well as loss of stability of the rope in the tape, the layer of the tape itself, and the entire body of the winding.

Multilayer winding is widely used in the production of composite materials, chemical fibers, in the textile industry, electrical and radio engineering, in the manufacture of paper, magnetic tape, film, etc. However, the existing theories of thread and isotropic tape winding are not applicable to the winding of a rubber-tube rope due to its structure.

A rubber-tube belt is a composite material with structural anisotropy and a certain symmetry of structure and properties, consisting of two components: rubber — a continuous component (matrix) and metal cables — a discrete component (reinforcement). In the works of prof. Kolosov L.V. [1] and his students, the above-mentioned tapes produced by domestic and foreign industry were studied and their promising designs were substantiated. Tabl. 1 shows brief technical characteristics of RTTs used in reel hoisting.

Table 1. Parameters of rubber-tube tapes

Parameter		Tape type						
		RTT-3150	RTT-4000	RTT-5000	RTT-6000	RTT-7600	RTT-8000	RTT-9100
Cable	Cable diameter, mm	8,250	8,000	10,500	11,500	10,000	12,900	11,500
	Cable pitch in the belt, mm	15,000	15,000	17,000	18,000	12,900	16,000	14,000
	Material model	Orthotropic						
	Elasticity modules by direction	10^5 MPa; $2 \cdot 10^5$ MPa						
	Poisson's ratios by direction	0,350; 0,004						
Rubber	Material model	Isotropic						
	Modulus of elasticity, MPa	3,000						
	Poisson's ratio	0,499						
	Total belt thickness, mm	22,500	23,000	25,500	26,500	20,000	22,000	22,000
	Permissible specific pressure of the rope on the rubber matrix, MPa	2,200	2,200	2,000	2,000	1,800	1,800	1,800
	Tangential stress strength, MPa	3,400	3,600	3,000	2,900	2,500	2,200	2,400

Problem's Formulation

From the analysis of the physical nature of the problem, it follows that the stiffness and deformation properties of the RTT layer in the winding depend on the parameters: $t_o = t/d$, $h_o = h/d$; m total number of cables; i — layer number in the package; j — total number of layers; E , $\nu_{резрез}$ — elastic modulus and Poisson's ratio of rubber; E_{mp1}, E_{mp2}, ν_{mp1}, ν_{mp2} — elastic moduli and Poisson's ratios of cables in the directions: index 1 corresponds to the direction along the cable, 2 — in the vertical direction transverse to the cable, and 3 — in the horizontal direction.

Macro- and micromechanical approaches are used to analyze composites [2]. In the macromechanical approach, the composite material is considered as a homogeneous anisotropic medium with symmetry of structure and properties that depend on the properties of the components. In the micromechanical approach, the stress-strain state (SSS) of regions commensurate with the characteristic sizes of the phases of the composite material is studied.

To find the values of the elastic constants that determine the properties of an equivalent anisotropic material under bulk SSS, a large number of physical experiments are required (the total number of elastic constants of the material other than zero is 36, the number of independent constants is 21). It is also necessary to take into account the conditions for fixing the RTT package at the boundaries (material constraint).

Therefore, we will limit ourselves to determining the integral stiffness characteristics of the RTT layers in the winding. Let us introduce the dimensionless integral characteristics:

– coefficient of longitudinal stiffness of the RTT layer

$$B_{mp} = \frac{\pi}{4} \cdot \frac{E_{mp1}}{E_{рез}} \cdot \frac{1}{t_o \cdot h_o}; \quad (1)$$

– coefficient of transverse stiffness of the RTT package layer

$$B = \frac{B_2 \cdot h}{m \cdot t \cdot E_{рез}}, \quad (2)$$

where B_2 — transverse stiffness of the RTT package layer;

– coefficient of expansion of the RTT package layer

$$K_{расш} = \frac{u_3}{u_2}, \quad (3)$$

where u_3 — horizontal average elongation (expansion) of the layer of the given package; u_2 — vertical average compression (shortening) of the layer.

Expression (1) is determined from the initial data, and research is required to find the coefficients (2) and (3).

Let us determine the values of the coefficients B and $K_{расш}$ depending on the RTT winding parameters: t_o, h_o, m, $E_{рез}$, $\nu_{рез}$, E_{mp1}, E_{mp2}, ν_{mp1}, ν_{mp2}, i, j. To solve this problem, we use the methods of computer finite element modeling, methods of planning a multifactorial experiment, and statistical processing of experimental data.

Formulation of the study purpose

The aim of the work is to develop a mathematical model of the stress-strain state of the winding body of a spool hoist with a rubber-tether rope.

Presenting main material

The finite element method is particularly successful in solving problems with complex stiffness properties. The most commonly used approach to building a finite element model is to specify displacement functions that require stresses to be expressed in terms of strains. In matrix form, Hooke's law takes the form:

$$\{\sigma\} = [E] \cdot \{\varepsilon\},$$

where $\{\sigma\}$, $\{\varepsilon\}$ — column vectors of stresses and strains; $[E]$ — material stiffness matrix of size 6× 6, which defines the general case of an anisotropic material.

Let's make the following assumptions:

1. In a multilayer winding, the RTT material is in a stress-strain state close to plane deformation.

2. The coefficients of transverse stiffness and expansion of the RTT package layer are represented as the product of two coefficients:

$$B = B_n \cdot f_n; \quad K_{расш} = k_{расш} \cdot w_n, \quad (4)$$

where B_n, $k_{расш}$ transverse stiffness and expansion coefficients of the package layer, taking into account only the geometry of the structure and the physical and mechanical properties of the components; f_n, w_n — coefficients of constriction of the RTT layer in the transverse direction, which take into account the edge effect when the RTT is in contact with the surface of the winding body. According to assumption 2, we divide the problem into two stages: determining B_n, $k_{расш}$ and f_n, w_n.

Definition B_n and $k_{расш}$. The finite element analysis was performed using the universal finite element modeling package ANSYS/ED 6.1. The finite element model of the RTT package was constructed from an orthotropic material based on the PLANE82 parabolic finite element with additional nodes:

$$\varepsilon_x = \frac{\sigma_x}{E_x} - \frac{\nu_{xy}}{E_x}\sigma_y - \frac{\nu_{xz}}{E_x}\sigma_z; \qquad \gamma_{xy} = \frac{\tau_{xy}}{G_{xy}};$$

$$\varepsilon_y = -\frac{\nu_{xy}}{E_x}\sigma_x + \frac{\sigma_y}{E_y} - \frac{\nu_{yz}}{E_y}\sigma_z; \qquad \gamma_{yz} = \frac{\tau_{yz}}{G_{yz}};$$

$$\varepsilon_z = -\frac{\nu_{xy}}{E_x}\sigma_x - \frac{\nu_{yz}}{E_y}\sigma_y + \frac{\sigma_z}{E_z}; \qquad \gamma_{zx} = \frac{\tau_{zx}}{G_{zx}}.$$

$$\sigma_x = \frac{E_x}{h}\left[1-\nu_{yz}^2\cdot\frac{E_z}{E_y}\right]\cdot\varepsilon_x + \frac{E_y}{h}\left[\nu_{xy}+\nu_{xz}\cdot\nu_{yz}\cdot\frac{E_z}{E_y}\right]\cdot\varepsilon_y + \frac{E_z}{h}\left[\nu_{xz}+\nu_{xy}\cdot\nu_{yz}\right]\cdot\varepsilon_z;$$

$$\sigma_y = \frac{E_y}{h}\left[\nu_{xy}+\nu_{xz}\cdot\nu_{yz}\cdot\frac{E_z}{E_y}\right]\cdot\varepsilon_x + \frac{E_y}{h}\left[1-\nu_{xz}^2\cdot\frac{E_z}{E_x}\right]\cdot\varepsilon_y + \frac{E_z}{h}\left[\nu_{yz}+\nu_{xz}\cdot\nu_{xy}\cdot\frac{E_y}{E_x}\right]\cdot\varepsilon_z;$$

$$\sigma_z = \frac{E_z}{h}\left[\nu_{xz}+\nu_{xy}\cdot\nu_{yz}\right]\cdot\varepsilon_z + \frac{E_z}{h}\left[\nu_{yz}+\nu_{xz}\cdot\nu_{xy}\cdot\frac{E_y}{E_x}\right]\cdot\varepsilon_y + \frac{E_z}{h}\left[1-\nu_{xy}^2\cdot\frac{E_y}{E_x}\right]\cdot\varepsilon_z;$$

$$\tau_{xy} = G_{xy}\cdot\gamma_{xy}; \qquad \tau_{yz} = G_{yz}\cdot\gamma_{yz}; \qquad \tau_{zx} = G_{zx}\cdot\gamma_{zx},$$

where τ_{xy}, τ_{yz}, τ_{zx} — tangential stresses; G_{xy}, G_{yz}, G_{zx} — shear module for planes parallel to the coordinate planes; γ_{xy}, γ_{yz}, γ_{zx} — elastic shear (angular) strains in the *xy*, *yz* and *zx* planes, respectively. ANSYS/ED 6.1 also provides a check for positive material certainty, which is a condition that the elastic constants of the material must satisfy:

$$h = 1-\nu_{xy}^2\cdot\frac{E_y}{E_x}-\nu_{yz}^2\cdot\frac{E_z}{E_y}-\nu_{xz}^2\cdot\frac{E_z}{E_x}-2\cdot\nu_{xy}\cdot\nu_{yz}\cdot\nu_{xz}\cdot\frac{E_z}{E_x}.$$

Fig. 1 shows the finite element model of a cable in a rectangular rubber matrix and the adopted *xyz* coordinate system: the *z-axis is* along the cable, the *y*- and *x-axes are along the* thickness and width of the RTR, respectively.

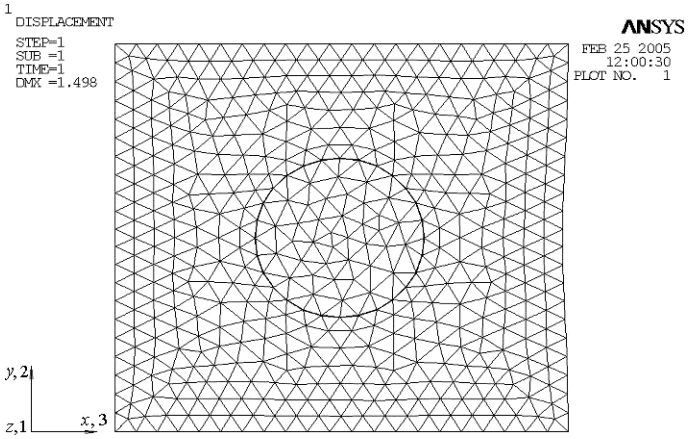

Fig. 1. Finite element model of a rubberized cable

Boundary conditions: the left edge of the rectangle has a symmetry condition, the bottom edge prohibits vertical movement, and the top edge has a prescribed movement.

To assess the validity of the first assumption, we compared the results of modeling the NDP for plane deformation (Fig. *2a*) and volumetric NDP (Fig. *2b*).

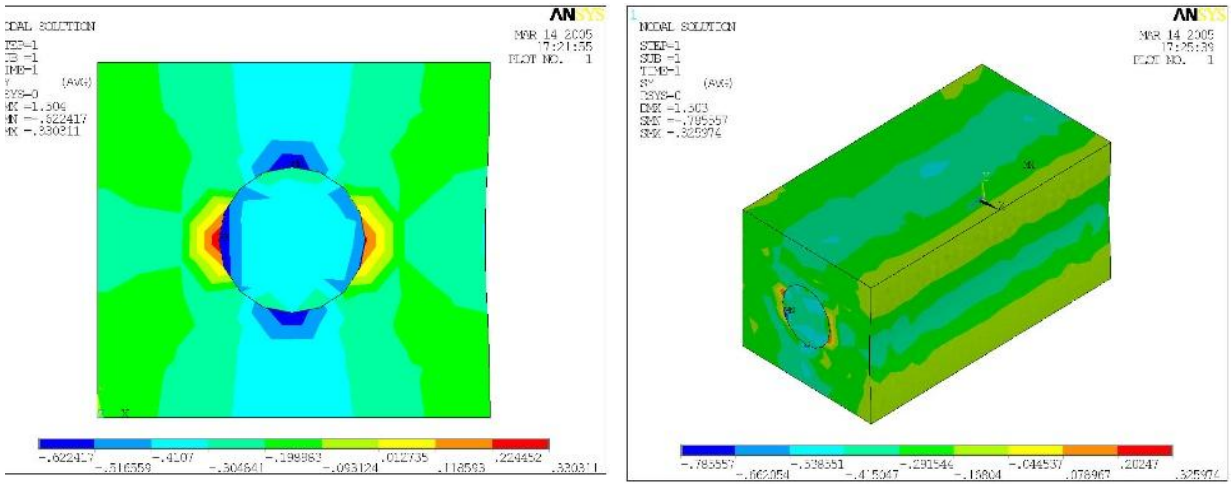

a b

Fig. 2. Stress fields a — for the case of plane deformation; b — for the three-dimensional problem

The results were processed using the following formulas

$$B = \frac{F_2}{m \cdot u_2 \cdot E_{рез}}; \tag{5}$$

$$K_{расш} = \frac{u_3 \cdot h_o}{u_2 \cdot t_o \cdot m}, \tag{6}$$

where F_2 — total vertical distributed load on the RTT package layer.

The calculation error when using the plane deformation hypothesis for the transverse stiffness coefficient was 0.06 %, and for the expansion coefficient — 3. This result confirmed the first assumption: the main design case for RTT — plane deformation.

To limit the size of the problem at a given calculation accuracy, the maximum step of the finite element mesh (Fig. 3 *a*, *b*), the minimum number of cables in the RTT layer (Fig. 3 *c*, *d*), and the minimum number of layers in the package (Fig. 3 *e*, *f*) are sequentially determined.

In the course of the experiment, the grid spacing was consistently reduced until the difference in the total vertical longitudinal loads on the *RTT*-F_2 package layer at the bottom edge in two consecutive calculations was less than 1 %. This was achieved with a grid spacing of 1 mm.

To determine the minimum number of cables in the layer, we compared the maximum tangential stresses in the rubber on the surface of the rightmost cable in two consecutive calculations. Thus, at m = 2, the error was 15 %, and at m = 8—2 %. The minimum number of layers in the package was determined in a similar way. Numerical experiments have shown that the stress-strain state does not depend on the number of layers. Further, one layer of RTT t = 8 was assumed in the calculations.

Taking into account the results of the reliability assessment, a numerical experiment was carried out: boundary conditions were set for the finite element model and the stress-strain state of the belt layer was determined. The results were processed using formulas (5) and (6). The geometric parameters of the RTT were varied. The results of computational experiments are summarized in Tabl. 2 and 3.

Table 2. Values of B_n from geometric parameters of RTT

h_o \ t_o	1,200	1,300	1,400	1,600	1,800	2,000
1,700	3,973	3,030	2,565	2,102	1,876	1,740
1,900	3,582	2,745	2,323	1,907	1,702	1,583
2,100	3,289	2,540	2,160	1,781	1,540	1,486
2,300	3,056	2,381	2,038	1,692	1,520	1,420
2,500	2,864	2,254	1,939	1,629	1,465	1,371
2,700	2,702	2,147	1,858	1,567	1,420	1,333

Table 3. Values of k_{pacu} from geometric parameters of RTT

h_o \ t_o	1,200	1,300	1,400	1,600	1,800	2,000
1,700	0,987	0,991	0,992	0,994	0,994	0,995
1,900	0,988	0,991	0,993	0,994	0,994	0,995
2,100	0,988	0,991	0,993	0,994	0,995	0,995
2,300	0,988	0,991	0,993	0,994	0,995	0,995
2,500	0,989	0,992	0,993	0,994	0,995	0,995
2,700	0,989	0,992	0,993	0,994	0,995	0,995

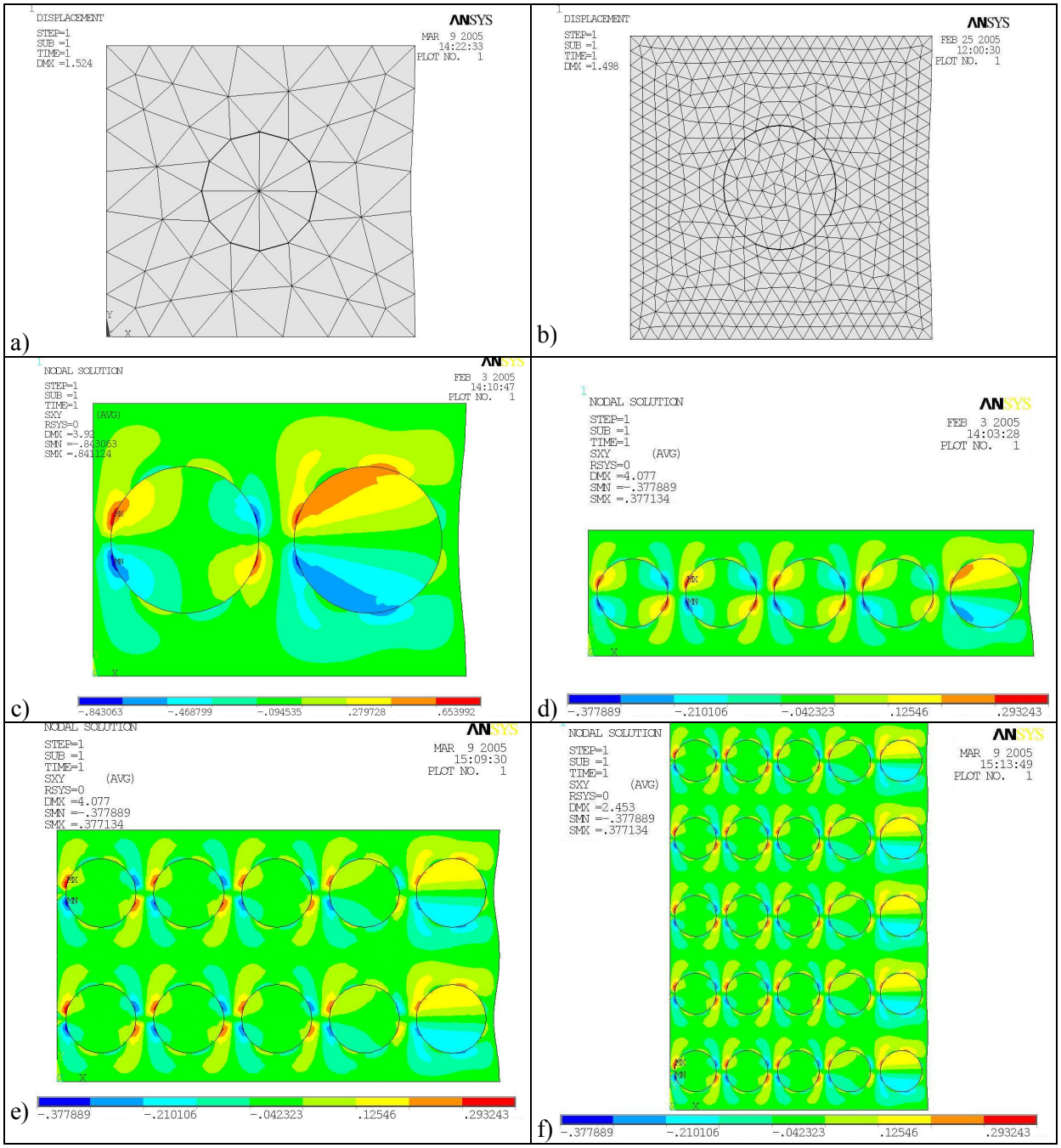

Fig. 3. Assessment of the reliability of the finite element model

As can be seen from tabl. 2, the values of the layer expansion coefficients are weakly dependent on the ratios of the parameters h_∂ and t_∂ and the average value $k_{расш} = 0,993$ can be taken in the future.

Taking h_∂, t_∂ for the variables, let us find an approximate function that connects them. Let us take the approximating polynomial for determining the transverse stiffness coefficients of the RTT package as follows

$$B_n = s_1 + s_2 \cdot \eta + s_3 \cdot \tau + s_4 \cdot \eta^2 + s_5 \cdot \eta \cdot \tau + s_6 \cdot \tau^2 . \quad (7)$$

here $\eta = \frac{1}{h_\partial - 1}$, $\tau = \frac{1}{t_\partial - 1}$ — new variables, whose values are determined by the data set, from tabl. 2;

vector of unknowns, determined by the least squares method by minimizing the squares of the deviations of the polynomial *B:*

$$\{s\}^T = \{s_1\ s_2\ s_3\ s_4\ s_5\ s_6\}. \quad (8)$$

$$\Delta = \sum_{i=1}^{m}\sum_{j=1}^{n}\left(-B_{i,j} + s_1 + s_2 \cdot \eta_i + s_3 \cdot \tau_j + s_4 \cdot \eta_i^2 + s_5 \cdot \tau_j \cdot \eta_i + s_6 \cdot \tau_j^2\right)^2, \quad (9)$$

where *m*, *n* — number of rows and columns in tabl. 2.

Let's find the partial derivatives of Δ. By equating them to zero, we obtain a system of equations to determine the coefficients of the vector $\{s\}$:

$$\begin{cases} \frac{\partial}{\partial s_1}\Delta = \sum_{i=1}^{m}\sum_{j=1}^{n}\left(-B_{i,j} + s_1 + s_2 \cdot \eta_i + s_3 \cdot \tau_j + s_4 \cdot \eta_i^2 + s_5 \cdot \tau_j \cdot \eta_i + s_6 \cdot \tau_j^2\right) = 0 \\ \frac{\partial}{\partial s_2}\Delta = \sum_{i=1}^{m}\sum_{j=1}^{n}\left(-B_{i,j} + s_1 + s_2 \cdot \eta_i + s_3 \cdot \tau_j + s_4 \cdot \eta_i^2 + s_5 \cdot \tau_j \cdot \eta_i + s_6 \cdot \tau_j^2\right) \cdot \eta_i = 0 \\ \frac{\partial}{\partial s_3}\Delta = \sum_{i=1}^{m}\sum_{j=1}^{n}\left(-B_{i,j} + s_1 + s_2 \cdot \eta_i + s_3 \cdot \tau_j + s_4 \cdot \eta_i^2 + s_5 \cdot \tau_j \cdot \eta_i + s_6 \cdot \tau_j^2\right) \cdot \tau_j = 0 \\ \frac{\partial}{\partial s_4}\Delta = \sum_{i=1}^{m}\sum_{j=1}^{n}\left(-B_{i,j} + s_1 + s_2 \cdot \eta_i + s_3 \cdot \tau_j + s_4 \cdot \eta_i^2 + s_5 \cdot \tau_j \cdot \eta_i + s_6 \cdot \tau_j^2\right) \cdot \eta_i^2 = 0 \\ \frac{\partial}{\partial s_5}\Delta = \sum_{i=1}^{m}\sum_{j=1}^{n}\left(-B_{i,j} + s_1 + s_2 \cdot \eta_i + s_3 \cdot \tau_j + s_4 \cdot \eta_i^2 + s_5 \cdot \tau_j \cdot \eta_i + s_6 \cdot \tau_j^2\right) \cdot \eta_i \cdot \tau_j = 0 \\ \frac{\partial}{\partial s_6}\Delta = \sum_{i=1}^{m}\sum_{j=1}^{n}\left(-B_{i,j} + s_1 + s_2 \cdot \eta_i + s_3 \cdot \tau_j + s_4 \cdot \eta_i^2 + s_5 \cdot \tau_j \cdot \eta_i + s_6 \cdot \tau_j^2\right) \cdot \tau_j^2 = 0 \end{cases} \quad (10)$$

We transform the system of equations (10) to the standard form:

$$[A] \cdot \{s\} = \{C\}, \quad (11)$$

where $\{s\}$ — column vector of unknowns (8); $[A]$ — main matrix of the system (11)

$$[A] = \begin{vmatrix} m \cdot n & \sum\sum \eta_i & \sum\sum \tau_j & \sum\sum \eta_i^2 & \sum\sum \eta_i \cdot \tau_j & \sum\sum \tau_j^2 \\ \sum\sum \eta_i & \sum\sum \eta_i^2 & \sum\sum \eta_i \cdot \tau_j & \sum\sum \eta_i^3 & \sum\sum \eta_i^2 \cdot \tau_j & \sum\sum \eta_i \cdot \tau_j^2 \\ \sum\sum \tau_j & \sum\sum \eta_i \cdot \tau_j & \sum\sum \tau_j^2 & \sum\sum \eta_i^2 \cdot \tau_j & \sum\sum \eta_i \cdot \tau_j^2 & \sum\sum \tau_j^3 \\ \sum\sum \eta_i^2 & \sum\sum \eta_i^3 & \sum\sum \eta_i^2 \cdot \tau_j & \sum\sum \eta_i^4 & \sum\sum \eta_i^3 \cdot \tau_j & \sum\sum \eta_i^2 \cdot \tau_j^2 \\ \sum\sum \eta_i \cdot \tau_j & \sum\sum \eta_i^2 \cdot \tau_j & \sum\sum \eta_i \cdot \tau_j^2 & \sum\sum \eta_i^3 \cdot \tau_j & \sum\sum \eta_i^2 \cdot \tau_j^2 & \sum\sum \eta_i \cdot \tau_j^3 \\ \sum\sum \tau_j^2 & \sum\sum \eta_i \cdot \tau_j^2 & \sum\sum \tau_j^3 & \sum\sum \eta_i^2 \cdot \tau_j^2 & \sum\sum \eta_i \cdot \tau_j^3 & \sum\sum \tau_j^4 \end{vmatrix};$$

$$\{C\} = \begin{vmatrix} \sum_{i=1}^{m}\sum_{j=1}^{n} B_{i,j} \\ \sum_{i=1}^{m}\sum_{j=1}^{n} B_{i,j}\cdot\eta_i \\ \sum_{i=1}^{m}\sum_{j=1}^{n} B_{i,j}\cdot\tau_j \\ \sum_{i=1}^{m}\sum_{j=1}^{n} B_{i,j}\cdot\eta_i^{\,2} \\ \sum_{i=1}^{m}\sum_{j=1}^{n} B_{i,j}\cdot\eta_i\cdot\tau_j \\ \sum_{i=1}^{m}\sum_{j=1}^{n} B_{i,j}\cdot\tau_j^{\,2} \end{vmatrix}$$ — column vector of free terms.

Using the Gaussian elimination method, a solution to the system of equations (11) with three digits of accuracy is obtained:

$$s^T = \{0,657 \quad 0,518 \quad 0,205 \quad -0,156 \quad 0,242 \quad 0,001\}. \tag{12}$$

Consequently, the coefficients of polynomial (7) are determined.

Definition f_n. The coefficient of transverse compression of the RTT layer takes into account the edge effect that occurs when the tape layer contacts the surface of the winding body.

For the finite element model, the edge effect is modeled in the boundary conditions by prohibiting vertical and horizontal movements of the lower edge of the RTT layer (constrained state).

The stress-strain state of a package made of RTT-3150 tape was investigated. In the numerical experiment, the number of tape layers in the package was varied and the transverse stiffness and expansion coefficients of each layer of the RTT package were determined, respectively, by formulas (4) and (5). As a result of the calculations, matrix [*B*] was obtained.

Let [*B*] be *a* matrix in which the element $B_{i,j}$ is the value of the transverse stiffness coefficient of layer *i* in a package with a total number of layers *j* (fig. 4).

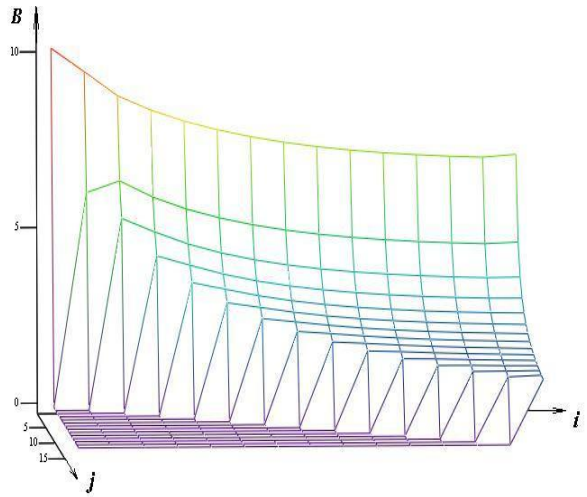

Fig. 4. Values of the transverse stiffness coefficient of layer *i* in a package with a total number of layers *j*

Obviously, the compression ratio *i* of the RTT layer in the transverse direction of a package with a total number of layers *j*

$$f_{i,j} = \frac{B_{i,j}}{B_n}, \tag{13}$$

where B_n — transverse stiffness coefficient of the RTT package determined by formula (7).

As a result of processing the experiment, we obtained the matrices $f_{i,j}$ and $w_{i,j}$, as well as their approximation functions with the coefficient vectors $\{k\}$ and $\{\kappa\}$, values of which were determined by the least-squares method.

$$f(i,j)=1+k_1\cdot k_2^{-(i-1)^{k3}}\cdot\left(1-k_4^{i-j}\right)+k_5\cdot k_6^{-(i-1)^{k7}}\cdot k_4^{i-j}; \quad (14)$$

$$k^T=\{3{,}123 \quad 1{,}888 \quad 0{,}632 \quad 1{,}292 \quad 5{,}106 \quad 1{,}572 \quad 0{,}807\}. \quad (15)$$

$$w(i,j)=1+\kappa_1\cdot\kappa_2^{-(i-1)^{\kappa3}}\cdot\left(1-\kappa_4^{i-j}\right)+\kappa_5\cdot\kappa_6^{-(i-1)^{\kappa7}}\cdot\kappa_4^{i-j}; \quad 16)$$

$$\kappa^T=\{-0{,}464 \quad 1{,}819 \quad 0{,}475 \quad 1{,}327 \quad -0{,}688 \quad 1{,}546 \quad 0{,}679\}. \quad (17)$$

Taking into account (6), (7), (12), (13), (14), and (15), we finally obtained an expression for the transverse stiffness coefficient *i* of the RTT layer in the transverse direction of a package with a total number of layers *j*:

$$B=\left(s_1+s_2\cdot\eta+s_3\cdot\tau+s_4\cdot\eta^2+s_5\cdot\eta\cdot\tau+s_6\cdot\tau^2\right)\cdot\left(1+k_1\cdot k_2^{-(i-1)^{k3}}\cdot\left(1-k_4^{i-j}\right)+k_5\cdot k_6^{-(i-1)^{k7}}\cdot k_4^{i-j}\right); \quad (18)$$

$$K_{крсш}=0{,}993\cdot\left(1+\kappa_1\cdot\kappa_2^{-(i-1)^{\kappa3}}\cdot\left(1-\kappa_4^{i-j}\right)+\kappa_5\cdot\kappa_6^{-(i-1)^{\kappa7}}\cdot\kappa_4^{i-j}\right). \quad (19)$$

Let us determine the discrepancy between the real values of the coefficients of transverse stiffness and layer expansion in the RTT package and the same coefficients obtained by formulas (18), (19). For this purpose, a numerical experiment similar to the definition of f_n: was conducted: boundary conditions were set for the finite element model and the stress-strain state of packages of RTT-2500, RTT-5000, and RTT-6000 tapes was investigated. In a numerical experiment with 30 layers in a package, the transverse stiffness and expansion coefficients of 1, 3, 5, 10, 15, 30 layers of the RTT package were determined using formulas (4) and (5). The comparison showed that the error in determining *B* and $K_{крсш}$ did not exceed 6 %.

In [1], the process of a transverse compression experiment of a RTT-2500 package 400 mm wide and 1000 mm long is presented. The tape segments were laid between the plates of a 500-ton hydraulic press in such a way that the cables were parallel to each other. During the loading process, the thickness and width of both the entire package and individual layers were measured.

The results of processing the experiments on changing the shape of the package are shown in Fig. 5, which shows that with an increase in the number of layers (package thickness), the difference between the relative deformation of the studied packages decreases. Thus, while the relative deformation of 2 and 10 layers differs significantly, this difference is insignificant for 8 and 10 layers. Such a deformation pattern is a consequence of the influence of edge effects caused by the friction forces of the belt layers on the surface of the press plates: with an increase in the height of the package, they have less effect on its deformation pattern. An increase in the number of layers above 10 does not lead to a significant difference from a 10-layer package, and with a number of layers above 10, the influence of edge effects can be neglected, i.e., the dependence of deformations on specific pressures can be assumed to be linear. A characteristic feature of the bundle deformation is the insignificance of the deformation in the direction of the axis of the cables, or rather, the bundle widening occurs without increasing its length.

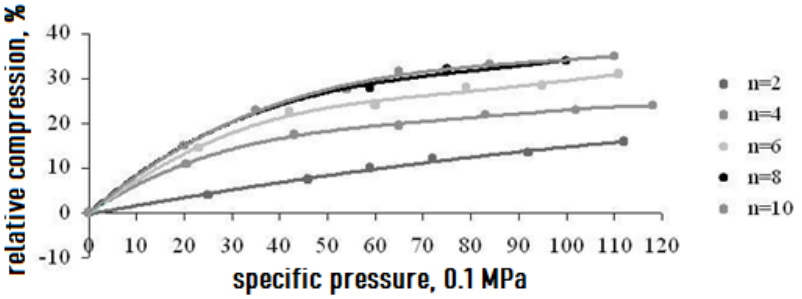

Fig. 5. Dependence of the relative compression $\varepsilon_в$ of the package on the specific pressure σ and the number of layers n

Tabl. 4 compares the experimental values of the transverse compression and expansion coefficients with the corresponding values of the numerical experiment.

Table 4. Values of transverse compression and expansion coefficients

Number of layers	Transverse stiffness factor		Expansion ratio	
	ANSYS B_A	Experimental $B_э$	ANSYS K_A	Experimental $K_э$
2	14,382	11,963	1,490	1,720
4	4,730	3,924	1,490	1,510
6	3,755	3,309	1,470	1,510
8	2,736	2,927	1,450	1,480
10	2,567	2,927	1,450	1,480

As you can see from the table, regardless of the number of layers, the results are satisfactory. The error does not exceed 20 %.

Conclusions

1. The main design case for the RTT package is plane deformation.
2. To limit the size of the problem with a given calculation accuracy, you can accept: the maximum step of the finite element mesh is 1 mm, the minimum number of cables is 8, and the number of layers in the package is 1. The error does not exceed 3 %.
3. The transverse stiffness coefficient of the package layer B_n for the given geometric parameters of the RTT can be determined using the approximating polynomial (7), where the values of the vector-column $\{s\}$ characterize the elastic constants of the RTT material.
4. In the absence of constriction $k_{расш}$ slightly dependent on the geometric parameters of the belt and can be taken as 0.993 with an accuracy of 1 %.
5. The matrix $[f_{i,j}]$ approximated by function (14), with $\{k\}$ given in (15).
6. The matrix $[w_{i,j}]$ is approximated by function (16), with $\{\kappa\}$ given in (17).
7. It is allowed to represent B as the product of B_n and $f_{i,j}$ (6). The error in the determination of B (18) does not exceed 6 % compared to the numerical experiment and 15 % compared to the physical experiment.

References

[1] Kolosov, D., Dolgov, O., Kolosov, A., (2013). The stress-strain state of the belt on a drum under compression by flat plates. *Annual Scientific-Technical Collection. Mining of Mineral Deposits*, pp. 351–357.

[2] Belmas, I., & Kolosov, D. (2011). The stress-strain state of the stepped rubber-rope cable in bobbin of winding. *Technical and Geoinformational Systems in Mining: School of Underground Mining 2011*, 211-214. Retrieved from https://www.researchgate.net/publication/330310760The_stress-strain_state_of_the_stepped_rubber-rope_cable_in_bobbin_of_winding.

[3] Belmas, I., Kogut, P., Kolosov, D., Samusia, V., & Onyshchenko, S. (2019). Rigidity of elastic shell of rubber-cable belt during displacement of cables relatively to drum. *E3S Web of Conferences*, *109*, 00005. https://doi.org/10.1051/e3sconf/201910900005.

[4] Zabolotnyi, K., Panchenko, O., & Zhupiiev, O. (2019). Development of the theory of laying a hoisting rope on the drum of a mining hoisting machine. *E3S Web of Conferences*, *109*, 00121. https://doi.org/10.1051/e3sconf/201910900121.

[5] Zabolotny, K., & Panchenko, E. (2010). Definition of rating loading in spires of multilayer winding of rubberrope cable. *New Techniques and Technologies in Mining – Proceedings of the School of Underground Mining*, 223-229. https://doi.org/10.1201/b11329-38.

[6] Zabolotnyi, K.S., Panchenko, O.V., Zhupiiev, O.L. & Polushyna, M.V. (2018). Influence of parameters of a rubber-rope cable on the torsional stiffness of the body of the winding. *Naukovyi Visnyk Natsionalnoho Hirnychoho Universytetu*, (5), 54-63. https://doi.org/10.29202/nvngu/2018-5/11.

Список використаної літератури

1. Kolosov D., Dolgov O., Kolosov A. The stress-strain state of the belt on a drum under compression by flat plates. *Annual Scientific-Technical Collection. Mining of Mineral Deposits*. 2013, №1. P. 351–357.
2. Belmas I., Kolosov D. The stress-strain state of the stepped rubber-rope cable in bobbin of winding. *Technical and Geoinformational Systems in Mining*. 2011. P. 211–214.
3. Belmas I., Kogut P., Kolosov D., Samusia, V., Onyshchenko, S. Rigidity of elastic shell of rubber-cable belt during displacement of cables relatively to drum. *E3S Web of Conferences*. 2019, 109, 00005. URL: https://doi.org/10.1051/e3sconf/201910900005.
4. Zabolotnyi K., Panchenko O., Zhupiiev O. Development of the theory of laying a hoisting rope on the drum of a mining hoisting machine. *E3S Web of Conferences*. 2019, 109, 00121. URL: https://doi.org/10.1051/e3sconf/201910900121.
5. Zabolotny K., Panchenko E. Definition of rating loading in spires of multilayer winding of rubber-rope cable. *New Techniques and Technologies in Mining – Proceedings of the School of Underground Mining*. 2010. P. 223–229.
6. Zabolotnyi K.S., Panchenko O.V., Zhupiiev O.L. Polushyna M.V. Influence of parameters of a rubber-rope cable on the torsional stiffness of the body of the winding. *Науковий вісник національного гірничого університету*. 2018, № 5. P. 54–63.

Надійшла до редколегії 22.11.2023